

See the Clear Benefits of Generic Contrast Agents
Same Quality. Lower Cost.



LEARN MORE

AJNR

This information is current as
of December 16, 2025.

Clinical Utility of [F18]-Fluciclovine PET/MRI for Differentiating True Progression from Treatment-Related Changes in Patients with Glioblastoma

Jana Ivanidze, Kellen Vo Vu, Rongwei Fu, Andrew Brandmaier, Laszlo Szidonya, Gagandeep Choudhary, Jay Starkey, Tony J. Wang, Michael Sisti, L. Guy McKhann, Sushant Puri, Marcus Konner, Michelle Roytman, Eaton Lin, Andrew Kuhn, Joseph R. Osborne, Philip E. Stieg, Kathryn Beal, Rohan R. Ramakrishna, Gagandeep Singh, Angela Lignelli-Dipple, Mikhail Doubrovin, Anh Huan Vo, Mary Welch, Fabio Iwamoto, Aya Haggiagi, Laura Donovan, Maria Diaz, Brian Gill, Benjamin Liechty, David J. Pisapia, Josh Walker, Rajiv S. Magge, Matthew Wood, Valentina Marulanda Corzo, Olabisi R. Sanusi, Ahmed Raslan, Aclan Dogan, Stephen Bowden, Sadek A. Nehmeh, Joshua Nickerson, Nadine Mallak, Amber Ruiz, Prakash Ambady, Ali Nabavizadeh and Ramon F. Barajas, Jr

AJNR Am J Neuroradiol published online 1 December 2025
<http://www.ajnr.org/content/early/2025/12/01/ajnr.A9120>

Clinical Utility of [F18]-Fluciclovine PET/MRI for Differentiating True Progression from Treatment-Related Changes in Patients with Glioblastoma.

Jana Ivanidze, Kellen Vo Vu, Rongwei Fu, Andrew Brandmaier, Laszlo Szidonya, Gagandeep Choudhary, Jay Starkey, Tony J. Wang, Michael Sisti, L. Guy McKhann, Sushant Puri, Marcus Konner, Michelle Roytman, Eaton Lin, Andrew Kuhn, Joseph R. Osborne, Philip E. Stieg, Kathryn Beal, Rohan R. Ramakrishna, Gagandeep Singh, Angela Lignelli-Dipple, Mikhail Doubrovin, Anh Huan Vo, Mary Welch, Fabio Iwamoto, Aya Haggiagi, Laura Donovan, Maria Diaz, Brian Gill, Benjamin Liechty, David J. Pisapia, Josh Walker, Rajiv S. Magge, Matthew Wood, Valentina Marulanda Corzo, Olabisi R. Sanusi, Ahmed Raslan, Aclan Dogan, Stephen Bowden, Sadek A. Nehmeh, Joshua Nickerson, Nadine Mallak, Amber Ruiz, Prakash Ambady, Ali Nabavizadeh, Ramon F. Barajas Jr.

ABSTRACT

BACKGROUND AND PURPOSE: Differentiating true progression from treatment-related changes in patients with glioblastoma (GBM) remains a major diagnostic challenge. Amino acid PET tracers such as [F18]-Fluciclovine provide biologically specific information, but clinical real-world validation across institutions is limited. We aimed to evaluate the clinical diagnostic performance of [F18]-Fluciclovine PET/MRI for distinguishing true progression from treatment-related change in patients with presumed GBM progression across 2 academic centers.

MATERIALS AND METHODS: In this retrospective, multi-institutional, IRB-approved study, we analyzed [F18]-Fluciclovine PET/MRI scans performed in patients with presumed GBM progression. All PET/MRI examinations were clinically indicated and performed as part of routine standard-of-care imaging. Clinical classification was based on histopathology or imaging and clinical follow-up. SUVmax was measured in enhancing lesions. Group comparisons were assessed with Mann-Whitney U tests. Diagnostic performance was evaluated using receiver operating characteristic (ROC) analysis, including derivation of an optimal cutoff using Youden's index and validation of the previously published diagnostic threshold of 4.66 (Nabavizadeh *et al.*). Subgroup analyses compared diagnostic performance across institutions.

RESULTS: Thirty-six patients with presumed GBM progression (Institution 1, n = 17; Institution 2, n = 19) provided 22 examinations classified as true tumor progression and 14 as treatment-related change. There were no significant differences in clinical or demographic study population characteristics between the two institutions. SUVmax was significantly higher in true tumor progression than in treatment-related change (median [interquartile range], 8.73 [5.86 - 10.83] versus 3.71 [1.70 - 4.67], $p < .01$). Combined ROC analysis demonstrated excellent diagnostic performance (AUC=0.90; 95% CI, 0.79-0.98). The optimal threshold of 5.7 yielded 86% sensitivity (0.70-0.99) and 86% specificity (0.64-0.99). Applying the published threshold of 4.66 produced similar results (AUC=0.90), with 91% sensitivity (0.71-0.99) and 71% specificity (0.42-0.92). A stratified analysis demonstrated comparable diagnostic performance across both institutions.

CONCLUSIONS: [F18]-Fluciclovine PET/MRI demonstrated high diagnostic accuracy for differentiating true GBM progression from treatment-related changes, with consistent SUVmax thresholds across 2 institutions. These findings support the generalizability of [F18]-Fluciclovine PET as a biologically specific adjunct to conventional MR imaging for patients with presumed GBM progression.

ABBREVIATIONS: [F18]-FACBC and [F18]-Fluciclovine = Trans-1-amino-3-[F18]-fluorocyclobutane-1-carboxylic acid; GBM = glioblastoma; IDH = Isocitrate Dehydrogenase; SUVmax = maximum standardized uptake value

Received October 8, 2025; accepted after revision November 19, 2025.

From the Department of Radiology, Weill Cornell Medicine, New York, NY (J.I., K.V.V., M.K., M.R., E.L., A.K., J.R.O., V.M.C., S.A.N.); School of Public Health, Division of Informatics, Clinical Epidemiology and Translational Data Science, Oregon Health & Science University, Portland, OR (R.F.); Department of Radiation Oncology, Weill Cornell Medicine, New York, NY (A.B., K.B.); Department of Radiology, Oregon Health & Science University, Portland, OR (L.S., G.C., J.S., J.N., N.M., R.F.B.); Department of Radiation Oncology, Columbia University Irving Medical Center, New York, NY (T.J.W.); Department of Neurological Surgery, Columbia University Irving Medical Center, New York, NY (M.S., G.M., B.G.); Department of Neurological Surgery, Oregon Health & Science University, Portland, OR (S.P., A.H.V., O.R.S., A.R., A.D., S.B.); Department of Neurological Surgery, Weill Cornell Medicine, New York, NY (P.E.S., R.R.R.); Department of Radiology, Columbia University Irving Medical Center, New York, NY (G.S., A.L.-D., M.D.); Department of Neurology, Columbia University Irving Medical Center, New York, NY (M.W., F.I., A.H., L.D., M.D.O.); Department of Pathology, Weill Cornell Medicine, New York, NY (B.L., D.J.P.); Department of Radiation Medicine and Department of Cell, Developmental and Cancer Biology, Oregon Health & Science University, Portland, OR (J.W.); Department of Neurology, Weill Cornell Medicine, New York, NY (R.S.M.); Department of Pathology, Oregon Health & Science University, Portland, OR (M.W.); Providence Brain & Spine Institute, Portland, OR 97225, United States (A.R., P.A.); Department of Radiology, University of Pennsylvania School of Medicine, Philadelphia, PA (A.N.) and the Advanced Imaging Research Center and Knight Cancer Center Translational Oncology Program, Oregon Health & Science University, Portland, OR (R.F.B.).

RFB is supported by a research grant from the National Institutes of Health National Cancer Institute under award No. R37CA288577

Please address correspondence to Ramon Francisco Barajas Jr, MD, Department of Radiology, Oregon Health & Science University 3181 SW Sam Jackson Park Road, Portland, OR 97239, USA. Email: BarajasLab@ohsu.edu

SUMMARY SECTION

PREVIOUS LITERATURE: Amino acid PET provides a biologically specific measure of brain tumor metabolism by assessing amino acid transport, offering advantages over conventional and perfusion MRI biomarkers. Amino acid PET radiotracers have demonstrated superior accuracy for differentiating true progression from treatment-related changes in glioblastoma (GBM). The most recent RANO and EANO consensus guidelines emphasize the clinical utility of amino acid PET for GBM diagnosis, radiotherapy planning, and treatment response assessment. [F18]-Fluciclovine, the only FDA-approved amino acid PET tracer in the United States, has shown promise for brain tumor imaging but remains underexplored outside of single-center or controlled research settings.

KEY FINDINGS: In this retrospective, multi-institutional cohort of 36 patients with presumed GBM progression, [F18]-Fluciclovine PET SUVmax accurately differentiated true progression from treatment-related changes (AUC = 0.90). Diagnostic performance was consistent across institutions, and prior bevacizumab exposure did not significantly alter accuracy, supporting the robustness of SUVmax as a clinically applicable biomarker.

KNOWLEDGE ADVANCEMENT: This study provides real-world, multi-institutional validation of [F18]-Fluciclovine PET/MRI for GBM response assessment, confirming reproducible diagnostic performance using a simple SUVmax threshold. These findings reinforce [F18]-Fluciclovine's potential as a biologically targeted adjunct to MRI, and demonstrate its feasibility for near-term integration into clinical neuro-oncology workflows.

INTRODUCTION

Glioblastoma (GBM, Isocitrate Dehydrogenase [IDH] wild type, World Health Organization [WHO] Grade 4 Astrocytoma) is the most aggressive primary brain malignancy in adults, characterized by rapid proliferation, diffuse infiltration, and poor prognosis despite maximal resection combined with subsequent Stupp protocol temozolomide based chemoradiotherapy (CRT) ¹. Gadolinium-based contrast enhanced MRI (Gd-MRI) remains the standard-of-care for response assessment but lacks biological specificity, as both tumor growth (true progression) and treatment-related inflammatory changes disrupt the blood-brain-barrier and produce similar enhancement patterns. Consequently, accurately distinguishing true progression from treatment-related change remains difficult and may lead to premature therapy discontinuation, delayed switching to second-line regimens, or unnecessary surgical interventions. Despite efforts to improve standardization, current response assessment criteria such as RANO 2.0 remains limited by its reliance on longitudinal characterization of nonspecific Gd-MRI features. As such, there is a critical need for biologically specific imaging biomarkers that improve upon the accuracy of Gd-MRI for GBM response assessment.

Physiology-based imaging approaches, including perfusion MRI and amino acid PET imaging, have emerged to address limitations of Gd-MRI. Dynamic susceptibility contrast (DSC) perfusion MRI derived cerebral blood volume (CBV) is commonly used in the clinical assessment of GBM due to its ability to detect microvascular proliferation, however the effects of CRT can confound interpretation. A meta-analysis reported pooled sensitivity of 0.84 and specificity of 0.78 for identifying GBM progression, with results limited by inter-institutional protocol variability and susceptibility artifacts. ² Dynamic contrast-enhanced (DCE) perfusion MRI represents a robust approach to assess intravascular volume (VP) and blood brain barrier permeability (Ktrans) and has been shown to be a helpful adjunct modality in assessment of GBM in the post treatment setting. While it is not affected by susceptibility artifact, DCE-MRI is affected by variability in institutional protocols similar to DSC-MRI.

Compared to perfusion MRI, amino acid PET imaging provides a more direct and biologically specific measure of lesional metabolic activity through assessment of amino acid transport³. Various amino acid PET radiotracers, including [F18]FET, [F18]FDOPA, and [C11]MET, have been developed and studied in the context of GBM response assessment. These radiotracers offer biological specificity and improved diagnostic accuracy for distinguishing true progression from treatment-related changes in GBM. ³⁻⁶ The most recent RANO/EANO consensus guidelines highlight its clinical utility in diagnosis, RT planning, and response assessment^{3,4,7}. Amino acid PET has shown clinical utility and cost-effectiveness in a variety of neuro-oncologic settings^{8,9}, and is increasingly being adopted in Europe. ¹⁰

Trans-1-amino-3-[F18]-fluorocyclobutane-1-carboxylic acid ([F18]-FACBC, also known as [F18]-Fluciclovine), is the only FDA-approved amino acid PET tracer currently available in the United States. Originally developed and approved for evaluating recurrent prostate cancer, [F18]-Fluciclovine has an excellent safety profile, and targets the ASCT2 and LAT1 transporters⁵. In recent years, [F18]-Fluciclovine has gained attention in the field of neuro-oncology as ASCT2 and LAT1 are overexpressed in GBM and other high-grade gliomas, as well as in brain metastases. ¹¹ In a recent prospective study by Nabavizadeh *et al.*, [F18]-Fluciclovine PET/MRI SUVmax cutoff threshold value of 4.66 demonstrated high diagnostic accuracy of 90% sensitivity and 83% specificity for distinguishing tumor progression from treatment effects, with an area under the curve (AUC) value of 0.86¹². However, broader clinical adoption of [F18]-Fluciclovine PET in neuro-oncology has been hindered by a paucity of real-world, multi-center data supporting its diagnostic performance in routine clinical settings. The scientific premise of this study is that [F18]-Fluciclovine PET/MRI, when applied in routine clinical practice, retains high diagnostic accuracy and reproducibility for identifying true progression in patients with GBM who present with new or enlarging contrast enhancement in the post-treatment setting. Therefore, we hypothesize that [F18]-Fluciclovine PET/MRI absolute

SUVmax measurements obtained in standard clinical workflows can reliably differentiate true tumor progression from treatment-related changes and serve as a valuable adjunct to Gd-MRI.

The purpose of this retrospective, two-institution study was to evaluate the clinical real-world performance of [F18]-Fluciclovine PET/MRI in differentiating tumor progression from treatment-related changes in patients with radiographically suspected (presumed) GBM progression. We demonstrate that [F18]-Fluciclovine SUVmax provides high diagnostic accuracy across institutions, reinforcing its potential role as a biologically targeted imaging biomarker in patients with GBM.

MATERIALS AND METHODS

Study Design and Patient Population

This retrospective study was conducted under institutional review board approved protocols at Institution 1 (Oregon Health & Science University) and Institution 2 (Weill Cornell Medicine). Informed consent was waived due to the retrospective nature of the study. We performed a multi-institutional cohort study to evaluate the clinical utility of [F18]-Fluciclovine PET/MRI in distinguishing true progression from treatment-related effects in patients with GBM (defined according to the World Health Organization 2021 classification) who previously received standard-of-care maximal safe resection followed by Stupp protocol radiation and concurrent temozolomide chemotherapy and adjuvant temozolomide.¹ Prior to undergoing [F18]-Fluciclovine PET/MRI, some patients were treated with bevacizumab for steroid-sparing management of cerebral edema or for treatment of a prior episode of disease progression. All patients underwent clinically indicated [F18]-Fluciclovine PET/MRI per institutional protocol, at the time of presumed disease progression as assessed by Gd-MRI RANO 2.0 (new contrast-enhancing lesions or lesions showing a $\geq 25\%$ increase in the sum of the products of the perpendicular diameters). All patients subsequently underwent maximal safe resection of the developing enhancing lesion or longitudinal Gd-MRI and clinical follow-up to define disease status. A STARD checklist is provided as **Supplementary Table 1**.¹³

PET/MRI Acquisition

[F18]-Fluciclovine radiotracer was acquired from commercial radiopharmaceutical vendors. All patients fasted for at least 4 hours prior to tracer administration. 185 ± 19 MBq (5 ± 0.5 mCi) at Institution 1 or 370 ± 37 MBq (10 ± 1.0 mCi) at Institution 2 of [F18]-Fluciclovine were administered intravenously. Imaging was performed using integrated PET/MRI systems: a GE SIGNA PET/MRI system (Institution 1 and Institution 2) or a Siemens Biograph mMR (Institution 2). At Institution 1, 3D-list mode PET acquisition was performed starting at injection for 60 minutes, and summed images were reconstructed from 40-50 minutes from injection and sent to PACS for clinical interpretation. At Institution 2, PET acquisition was performed in 3D-list mode from 30-50 minutes post-injection, and the 20-minute dataset was reconstructed and sent to PACS for clinical interpretation. At both institutions, standard iterative reconstruction algorithms with atlas- or Zero-Echo Time image-based attenuation correction were applied.

Brain MRI without and with gadolinium-based contrast was performed concurrently with the PET/MRI or within 2 weeks of the PET/MRI using institutional clinical brain tumor imaging protocols. Brain Tumor Imaging Protocol sequences included pre- and postcontrast axial 3D T1-weighted and axial T2-weighted FLAIR¹⁴. Post gadolinium-based contrast (0.1 mmol/kg) T1-weighted imaging was performed 8-12 minutes following injection. Key MRI sequence parameters are listed in **Supplemental Table 2**.

Imaging Analysis

PET/MRI image analysis was conducted using MIM Software (V7.1, Institution 1) or Siemens syngo.via MM Oncology (VB 50, Institution 2). Volumes of interest (VOIs) were manually placed on the postcontrast T1-weighted MRI over areas of new or enlarging enhancement. The VOI was used to extract PET SUVmax values from co-registered [F18]-Fluciclovine PET static images. VOI placement was performed by a board-certified neuroradiologist at each site blinded to clinical outcomes.

Clinical Diagnostic Criteria

Clinical classification of each case, as true progression or treatment-related changes, was based on histopathologic confirmation (when available) or serial imaging follow-up over at least 3 months or until death, consistent with the framework outlined in RANO 2.0^{6,15}. For patients undergoing resection or biopsy following PET/MRI, biopsy tissue provided for a clinical diagnosis of viable tumor or treatment-related changes as characterized on histopathology by a board-certified neuropathologist. For patients undergoing serial Gd-MRI to establish disease status, lesions that demonstrated continued enlargement or necessitated change in management were classified as true progression. Lesions that remained stable or regressed without therapeutic change were classified as treatment-related changes.

Statistical Analysis

Patient characteristics were summarized using descriptive statistics. Group differences in SUVmax were evaluated using Mann Whitney U test, a nonparametric test for two independent samples. Demographic and clinical characteristics between institutions were compared using the Mann-Whitney U test for continuous variables and Fisher's exact test or chi-square test for categorical variables, as appropriate. For patients with multiple imaging timepoints, only the first episode of presumed disease progression was included in the analysis to ensure independence of included scans and avoid correlation between repeated scans. Receiver operating characteristic (ROC) analysis was used

to evaluate diagnostic performance, with the area under the curve (AUC) along with 95% confidence intervals derived by bootstrap resampling with 10,000 iterations. Youden's J statistic was used to identify the optimal SUVmax cutoff for differentiating true tumor progression from treatment-related changes. Additionally, we evaluated the diagnostic performance of the previously published SUVmax threshold of 4.66, as reported in a prospective, histopathologically confirmed GBM cohort by Nabavizadeh *et al.*¹² and qualitatively compared its performance within our optimal cohort-specific threshold to assess consistency and generalizability across studies. A p-value less than .05 was considered statistically significant. Statistical analyses were performed using GraphPad Prism (Version 10.6.0, GraphPad Software, La Jolla, CA), Statistics Kingdom (Version August - November 2025, Statistics Calculators, Melbourne, Australia)¹⁶, and Stata/SE 16.1 (StataCorp LLC, college Station, TX). Pre-planned sample size justification was not performed.

RESULTS

Patient Cohort and Clinical Classification

All retrospectively identified patients with presumed GBM disease progression with [F18]-Fluciclovine PET/MRI were included in this cohort. In total, 36 patients were identified (**Table 1**). Seventeen scans were performed at Institution 1 and 19 at Institution 2. One patient at each institution had two separate episodes of presumed disease progression, but only the first was included in the analysis. Twenty-two PET/MRI examinations were classified as true tumor progression and 14 were classified as treatment-related changes, based on histopathology or radiographic and clinical follow-up. The follow-up time to establish diagnosis was significantly shorter at Institution 1 ($P = .01$; **Table 1**). Otherwise, clinical and demographic characteristics, including age, sex, MGMT promoter methylation status, number of prior therapies, proportion of patients who received Bevacizumab or other therapies, time from completion of radiotherapy to PET did not differ significantly between the two institutions (**Table 1**). The minimum follow up time after [F18]-Fluciclovine PET/MRI imaging to establish diagnosis within our cohort for patients without histological diagnosis of disease status was 0.6 months as result of subsequent death. However, length of follow up time did not preclude a clinical diagnosis of either true tumor progression or treatment-related changes.

Cohort Wide SUVmax Stratified by Clinical Outcome

Lesions classified as true progression demonstrated significantly higher SUVmax values compared to those identified as treatment-related changes ($p < .01$; **Figure 1**). **Figure 2** illustrates representative PET/MRI images from cases of both true progression and treatment-related changes (1 patient from each institution). Median SUVmax values of true progression ($P = .02$ and treatment-related changes at Institution 1 were overall significantly higher than Institution 2 ($P = .03$); **Table 2**).

Diagnostic Performance of SUVmax

ROC analysis revealed SUVmax had excellent diagnostic performance in distinguishing true progression from treatment-related changes, with an AUC of 0.90 (95% CI: 0.79 - 0.98). The optimal SUVmax threshold for this combined 2-institution cohort was 5.7, which yielded a sensitivity of 0.86 (95% CI: 0.70–0.99) and specificity of 0.86 (95% CI: 0.64–0.99) (**Figure 3**). A stratified analysis by institution demonstrated similar diagnostic performance (**Table 3, Supplementary Table S3**). The diagnostic performance of the previously published SUVmax threshold from Nabavizadeh *et al.* was evaluated in our combined 2-institution cohort. This threshold of 4.66 yielded similar performance with AUC of 0.90 (95% CI 0.79–0.98), sensitivity of 0.91 (95% CI: 0.71–0.99), and specificity of 0.71 (95% CI: 0.42–0.92). A subgroup of the 11 patients with histopathological confirmation of disease status ($N = 6$ true progression and $N = 5$ treatment related changes) demonstrated a similar diagnostic performance with an AUC of 0.87 (95% CI 0.60–1.00), sensitivity of 0.67 (95% CI: 0.29–0.96), and specificity of 1.0 (95% CI: 0.48–1.00) using the optimal SUVmax threshold of 5.7.

Table 1: Clinical and Demographic Characteristics of the Study Population. Continuous variables were compared using the Mann-Whitney U test; categorical variables were compared using Fisher's exact test or chi-square test, as appropriate. Number of prior systemic therapies, 1= only Stupp CRT received prior to Fluciclovine PET, 2= Stupp CRT and a second line of therapy received for episode recurrence prior to Fluciclovine PET, ≥ 3 = Stupp CRT and a third line of therapy received for second episode recurrence prior to Fluciclovine. Values are reported as median (IQR) unless otherwise specified; the overall range of time from completion of radiotherapy to PET/MRI across the cohort was 5-23 months. Duration of follow-up is from time of Fluciclovine PET imaging to clinical establishment of diagnosis measured in months.

Characteristic	Institution 1 (N = 17)	Institution 2 (N = 19)	p-value	Total (N = 36)
Age, years (mean, range)	55 (35-78)	58 (35 - 83)	0.51	56 (35–83)
Sex, n (%) - Female	6/17 = 35%	8/19 = 42%	0.74	14/36 = 39%
IDH wildtype	17/17 = 100%	19/19 = 100%	–	36/36 = 100%
MGMT promoter methylated (%)	8/17 = 47%	8/19 = 42%	1.0	16/36 = 44%
MGMT promoter methylated with Disease Progression (%)	4/12 = 33%	3/10 = 30%	1.0	7/22
Time from completion of most recent RT to PET, median (IQR), months	6 (5 – 10)	10 (5 – 23)	0.09	9 (5 – 13)
Number of prior systemic therapies, n (%)				
– 1 (Stupp protocol CRT only)	11/17 = 64%	8/19 = 42%	0.36	19/36 = 53%
– 2	4/17 = 24%	6/19 = 32%		10/36 = 28%

– ≥3	2/17 = 12%	5/19 = 26%		8/36 = 22%
Bevacizumab prior to PET, n (%)	4/17 = 24%	5/19 = 26%	1.00	9/36 = 25%
Tumor Treatment Fields prior to PET, n (%)	5/17 = 29%	5/19 = 26%	0.83	10/36 = 28%
Immunotherapy (pembrolizumab or vaccine) prior to PET, n (%)	1/17 = 6%	6/19 = 32%	0.10	7/36 = 19.4
Lomustine prior to PET, n (%)	3/17 = 18%	3/19 = 16%	1.00	6/36 = 17%
Erdafitinib prior to PET, n (%)	1/17 = 6%	1/19 = 5%	1.00	2/19 = 6%
Number of RT courses prior to PET				
–1	14/17 = 82%	15/19 = 79%	1.00	29/36 = 81%
–2	3/17 = 18%	4/19 = 21%		7/36 = 19%
Reference Standard for Diagnosis				
Histopathologic confirmation, n (%)	6/17 = 35%	6/19 = 32%	1.00	12/36 = 33%
Longitudinal follow-up, n (%)	11/17 = 65%	13/19 = 68%		24/36 = 67%
Clinical Classification				
–Progression	12 (71%)	10 (53%)	0.32	22 (61%)
–Treatment-related change	5 (29%)	9 (47%)		14 (39%)
Duration of follow-up, median (IQR), months	2 (1 – 3)	4 (2 – 4)	0.01	2 (1 – 4)

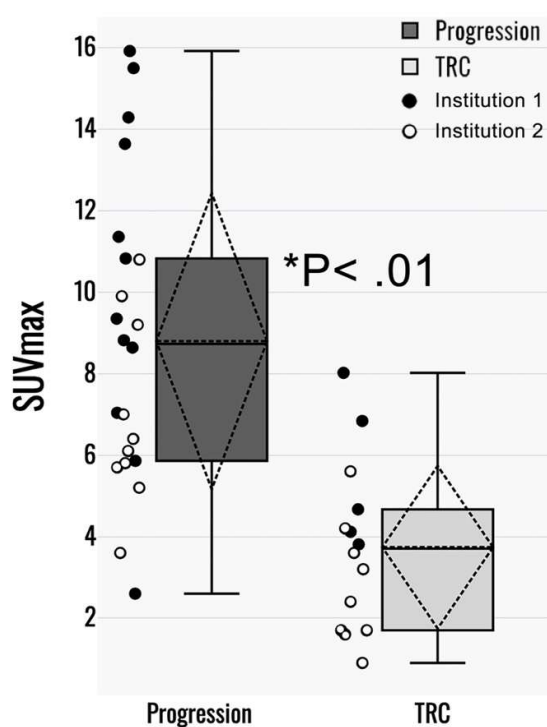


FIG 1. F18]-Fluciclovine avidity stratified by disease status. Combined cohort-wide analysis of [F18]-Fluciclovine SUVmax stratified by true tumor progression vs treatment-related changes in 36 cases of presumed GBM progression following CRT. SUVmax in the progression cohort was observed to be significantly higher when compared to TRC ($P < .01$).

Table 2: [F18]-Fluciclovine SUVmax by Subgroup and Institution. Median and interquartile range are provided along with p-values indicating statistical significance (Mann Whitney U test for group comparisons).

	Progression	Treatment-Related Changes	p-Value
Combined	8.73 (5.86 - 10.83) N= 22	3.71 (1.7 - 4.67) N= 14	< .01
Institution 1	10.09 (7.84 - 13.96) N= 12	4.67 (4.12 - 6.84) N= 5	.02
Institution 2	6.25 (5.7 - 9.2) N= 10	2.4 (1.7 - 3.6) N= 9	< .01

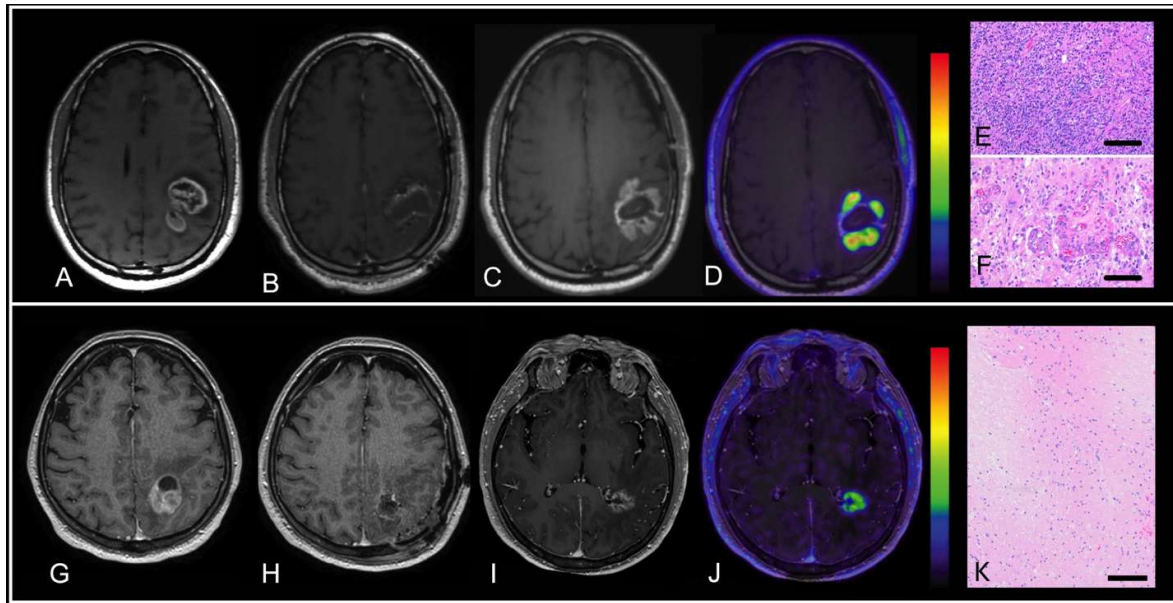


FIG 2. Clinical Case Examples of [F18]-Fluciclovine PET/MRI Response Assessment. Longitudinal contrast enhanced T1-weighted imaging in true disease progression (Top Row) and treatment-related changes (Bottom Row). True Disease Progression: Pre-operative imaging from a 53-year-old man with left peri-rolandic enhancing mass (A) who underwent maximal safe surgical resection (B) which confirmed MGMT unmethylated GBM. The patient subsequently was treated with standard-of-care CRT. New enhancement about the resection cavity margins, representing presumed disease progression, (C) occurred 6 months following completion of CRT. [F18]-Fluciclovine PET/MRI imaging (D) fused with T1-post contrast imaging demonstrated heterogeneously elevated [F18]-Fluciclovine avidity throughout the enhancing mass, with an SUVmax of 9.9, suspicious for true tumor progression. Subsequent surgical resection clinically validated disease status which was evidenced by marked hypercellularity (E) and microvascular proliferation (F). Treatment Related Changes: Pre-operative imaging from a 62-year-old man with a left peri-rolandic enhancing mass (G) who underwent maximal safe surgical resection (H) which confirmed MGMT unmethylated GBM. A new enhancing lesion inferior and medial to the resection cavity in the peri-atrial white matter, representing presumed disease progression, (I) occurred 16 months following completion of CRT necessitated [F18]-Fluciclovine PET/MRI imaging (J) fused with T1-post contrast imaging. Homogenous [F18]-Fluciclovine avidity throughout the enhancing mass demonstrated focal SUVmax of 4.7 suggested treatment related changes. Subsequent surgical resection (K) clinically validated disease status which was evidenced by necrotic parenchyma (left), minimally atypical glial cells (middle), hyalinized blood vessels vasculopathy (not shown). Scale bar in PET/MRI fused images: PET Rainbow color scale, set to maximum SUV 0-7.

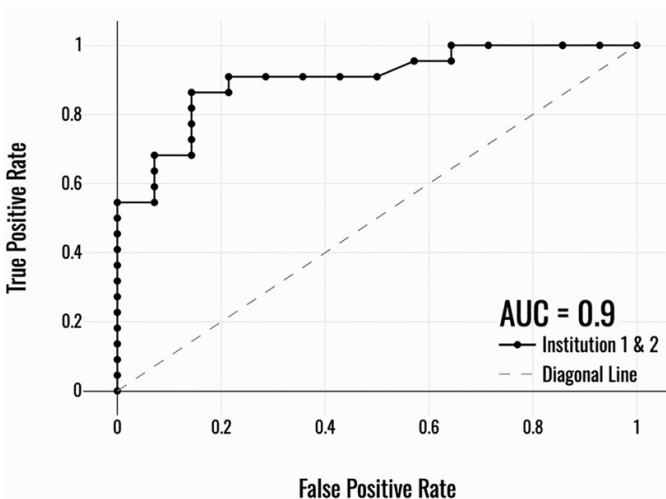


FIG 3. Receiver Operating Characteristic Curve Analysis of [F18]-Fluciclovine PET/MRI SUVmax. Combined cohort wide analysis of [F18]-Fluciclovine SUVmax demonstrated an area under the curve (AUC) of 0.9. Youden's J analysis provided an optimal SUVmax threshold of 5.7, with diagnostic testing yielding sensitivity of 0.86, specificity of 0.86, and accuracy of 0.86, suggesting excellent diagnostic discrimination capabilities and supporting its clinical utility as an imaging biomarker for differentiating true tumor progression from treatment related changes.

Table 3: Diagnostic Performance of [F18]-Fluciclovine SUVmax for Differentiating Treatment Related Changes from Glioblastoma Progression. Reported as calculated value (95% confidence interval). AUC= Area Under the ROC Curve.

	SUVmax Threshold	AUC	Sensitivity	Specificity	Accuracy
Combined	5.70	0.90 (0.79-0.98)	0.86 (0.70-0.99)	0.86 (0.64-0.99)	0.86 (0.71-0.97)
Nabavizadeh <i>et al</i> ⁸	4.66	0.90 (0.79-0.98)	0.91 (0.71-0.99)	0.71 (0.42-0.92)	0.83 (0.68-0.92)
Institution 1	8.64	0.87 (0.67-1.00)	0.75 (0.43-0.95)	1.00 (0.48-1.00)	0.82 (0.57-0.96)
Institution 2	5.70	0.96 (0.86-1.00)	0.80 (0.49-0.94)	1.00 (0.70-1.00)	0.9 (0.74-0.99)

Impact of Bevacizumab Exposure and Other Therapies

Nine patients (24%) had received bevacizumab prior to PET. Overall diagnostic accuracy did not differ between patients with and without prior bevacizumab exposure (89% vs 86%, Fisher's exact $p = 1.0$). Likewise, no significant difference was observed in SUVmax values between patients with and without prior bevacizumab exposure, irrespective of outcome ($P > .37$). Within the bevacizumab-treated subgroup ($N = 9$), SUVmax values trended higher in progression ($N = 6$) compared to treatment-related change ($N = 3$), with a SUVmax 7.35 (6.40 - 8.82) vs 3.20 (2.80 - 3.50), however this difference did not reach statistical significance ($p = 0.10$), likely due to small sample size. In the non-bevacizumab cohort ($N = 27$), the separation between progression ($N = 17$) and treatment-related change ($N = 10$) was robust (9.27 (5.83 - 12.23) vs 4.12 (1.7 - 5.13), $p < 0.001$). Mean and standard deviation for the overall cohort and subgroups SUVmax values are provided in **Supplementary Table 4**. SUVmax values were not significantly different when stratified by other therapies received prior to [F18]-Fluciclovine PET/MRI (bevacizumab, tumor treatment fields, pembrolizumab, or lomustine, **Table 1**).

DISCUSSION

In this retrospective, multi-institutional cohort study, we investigated the real-world diagnostic performance of [F18]-Fluciclovine PET/MRI for differentiating true tumor progression from treatment-related changes in patients with clinically presumed GBM progression. Our results suggest that SUVmax is significantly elevated in patients with true progression compared to those with treatment-related changes, and that a SUVmax threshold can reliably discriminate between these disease processes with high diagnostic accuracy. Furthermore, SUVmax performed as a robust clinical metric, supporting its applicability in real-world, multi-center clinical settings as a simple, threshold-based approach to facilitate clinical decision-making. Taken together, these findings suggest that [F18]-Fluciclovine PET/MRI offers clinically valuable, biologically specific information to aid in response assessment after standard-of-care CRT. With continued clinical validation in larger, prospective cohorts, [F18]-Fluciclovine PET/MRI could become a valuable diagnostic tool capable of complementing Gd-MRI for evaluating presumed disease progression in patients with GBM.

Our study suggests that [F18]-Fluciclovine SUVmax accurately differentiates true GBM progression from treatment-related changes, with an AUC of 0.90 and optimal diagnostic threshold of 5.7. These results are consistent with the prospective findings by Nabavizadeh *et al.*, who reported a SUVmax threshold of 4.66 with high diagnostic accuracy (AUC = 0.86)¹². Our ability to replicate their performance metrics in a real-world setting across two academic institutions, including acquisition parameters and analytical software packages, supports the robustness of [F18]-Fluciclovine SUVmax as a clinically prudent biomarker under heterogeneous imaging conditions. Although prior amino acid PET studies have explored ratios such as tumor to background ratio (TBR) or alternative metrics such as SUVpeak, we focused on SUVmax, a metric that has demonstrated excellent diagnostic performance for [F18]-Fluciclovine in GBM, particularly in multi-institutional settings where acquisition protocols vary. Importantly, the close concordance of threshold values across studies suggests that a standardized cutoff may be feasible for broader clinical implementation, reducing variability and interpretation bias.

Notably, while the two institutions differed in their absolute SUV distributions and optimal cutoffs (Institution 1: 8.64; Institution 2: 5.70), diagnostic accuracy remained consistently high at both sites (AUC 0.87–0.96). This finding highlights that inter-site technical or biological factors may shift absolute SUV, while the discriminatory capacity of [F18]-Fluciclovine PET remains preserved. The robustness of AUC across centers reinforces the generalizability of [F18]-Fluciclovine PET across clinical environments.

Although bevacizumab can alter the imaging appearance of enhancing lesions by reducing vascular permeability⁶, our data suggest that prior bevacizumab exposure does not substantially diminish the diagnostic performance of [F18]-Fluciclovine PET. While the bevacizumab-treated subgroup was small, we observed a similar separation of SUVmax values between progression and treatment-related change as in the non-bevacizumab cohort, supporting the potential robustness of Fluciclovine PET even in this clinically challenging setting.

Our findings are comparable to reports using O-(2-[[F18]]fluoroethyl)-L-tyrosine (FET) PET, which is more widely used in Europe and has similarly demonstrated high diagnostic accuracy for GBM progression. In this context, PET RANO 1.0, and its recent update, PET RANO 2.0, have attempted to formalize the integration of amino acid PET imaging into standardized response assessment frameworks,

emphasizing the need for reproducible, biologically specific imaging biomarkers to complement conventional MRI³. However, FET studies have reported a relatively wide range of optimal thresholds and diagnostic performance across institutions, with published TBR cutoffs ranging from ~1.9 to 3.7 and specificity varying considerably¹⁷⁻²⁰. By contrast, both our two-institution cohort and the single-institution experience from Nabavizadeh *et al.*¹² demonstrate highly consistent SUVmax thresholds and diagnostic accuracy for [F18]-Fluciclovine, suggesting greater robustness and generalizability across clinical settings. In either case, the use of static acquisition and clinically prudent SUVmax thresholds makes amino acid PET imaging more readily applicable in routine clinical workflows. Moreover, [F18]-Fluciclovine is FDA-approved and commercially available in the United States, offering logistical advantages for rapid clinical adoption in neuro-oncology practices.

In addition to confirming diagnostic performance, our study underscores the limitations of existing imaging methods. Conventional Gd-MRI features, as reflected in RANO 2.0 criteria, remain non-specific, particularly in the early post-treatment period. Although RANO 2.0 introduces updated criteria to improve standardization in Gd-MRI based GBM response assessment, Gd-MRI diagnostic accuracy for distinguishing true progression from treatment-related changes remains limited, with reported accuracies ranging from 50–70% depending on timing and imaging context²¹. As outlined in RANO 2.0, MRI-based assessment remains the clinical standard. Our findings suggest amino acid PET provides a complementary biologically specific marker that may refine response evaluation. DSC-MRI derived CBV is widely used to assess tumor vascularity. However, its diagnostic accuracy for differentiating GBM progression from treatment-related changes is variable, with reported sensitivities and specificities typically ranging from 60–85%². FDG-PET has historically shown limited diagnostic accuracy for GBM response assessment due to high physiologic glucose uptake in normal gray matter which reduces tumor-to-background contrast, complicating interpretation²². Prior investigations have attempted to address this marked limitation using delayed imaging protocols. Delayed imaging methodology acquires FDG-PET imaging 3–4 hours post-injection and may improve lesion conspicuity by allowing background cortical activity to decline²³. However, even with delayed imaging, reported diagnostic accuracy remains variable, with sensitivities and specificities generally in the 60–80% range, limiting its clinical utility compared to amino acid PET tracers²⁴.

This study seeks to advance the field of neuro-oncologic imaging by providing real-world, multi-institutional, evidence supporting the clinical utility of [F18]-Fluciclovine PET/MRI for GBM response assessment. By demonstrating high diagnostic accuracy across two centers despite modest inter-site SUV shifts, this work demonstrates that [F18]-Fluciclovine PET offers a robust, biologically specific biomarker that can be seamlessly integrated into routine clinical workflows. Although performed at tertiary academic centers with PET/MRI capabilities, all examinations were performed and interpreted within standard clinical practice rather than under a controlled research protocol, reflecting practical real-world diagnostic implementation. Unlike other imaging modalities that require complex kinetic modeling or suffer from limited specificity, [F18]-Fluciclovine PET/MRI enables straightforward, quantitative interpretation using static imaging, lowering the barrier for broader clinical adoption. These findings align with and extend prior prospective work, moving the field closer to establishing standardized, PET-based criteria for post-treatment response assessment in GBM. Future multi-center studies incorporating PET/CT platforms, community practice settings, and cost-effectiveness analyses will be important to confirm our results and address broader community-based implementation strategies.

The clinical imaging retrospectively assessed in this study was conducted using [F18]-Fluciclovine, which is FDA-approved for imaging suspected recurrent prostate cancer. Its use for brain tumors is off-label; however, both participating academic centers have achieved consistent insurance reimbursement for neuro-oncologic indications, supporting the practical feasibility of implementation in routine clinical practice. In the absence of any amino-acid PET tracers formally approved by the FDA for brain tumor evaluation in the United States, [F18]-Fluciclovine provided a practical and reimbursable option for addressing the diagnostic uncertainty frequently encountered in patients with GBM. Its use in this context underscores the feasibility of incorporating [F18]-Fluciclovine PET in routine neuro-oncology workflows and highlights the unmet need for expanded regulatory approval of dedicated brain tumor amino acid tracers. These findings and implementation experiences are consistent with the recent RANO/EANO consensus recommendations, which emphasize the expanding clinical utility of amino acid PET for glioma evaluation and the importance of establishing harmonized protocols and regulatory pathways.³

This study has several limitations. First, the retrospective design introduces potential selection bias, and histopathologic confirmation was not available for all cases. In some patients, true progression or treatment-related changes were inferred from longitudinal imaging and clinical follow-up, which may be imperfect surrogates introducing the possibility of verification bias and optimism in the reported diagnostic performance metrics. Second, the sample size, while larger than prior single institution studies, remains modest, limiting statistical power and subgroup analyses. Third, imaging protocols, though harmonized to the extent possible, varied slightly across institutions in terms of acquisition time window and post-processing software. Moreover, because most patients in our cohort underwent imaging in the intermediate-to-late post-treatment period (median 9 months after completion of chemoradiation), diagnostic performance estimates may not directly extrapolate to the early post-therapy interval (<6 months), when treatment-related change is most prevalent^{1,25,26}. Prior amino acid PET studies have also demonstrated that diagnostic accuracy and optimal thresholds vary according to the post-treatment interval, with the early post-CRT period posing the greatest interpretive challenge²⁷. Finally, we focused on SUVmax within the lesion and did not assess dynamic PET parameters or serial PET RANO response assessment, which may offer additional diagnostic value in

future prospective studies.

CONCLUSIONS

In conclusion, our retrospective, multi-institutional study demonstrates that [F18]-Fluciclovine PET/MRI, using a SUVmax threshold, can accurately differentiate true tumor progression from treatment-related changes, with high sensitivity and specificity consistent across institutions. These findings support the clinical utility of [F18]-Fluciclovine PET as a biologically specific adjunct to conventional Gd-MRI. This provides an imaging tool that may improve diagnostic confidence for GBM response assessment. Moreover, given that [F18]-Fluciclovine is FDA-approved and reimbursed for other oncologic indications, its established clinical availability facilitates near-term adoption for neuro-oncology practice in the United States.

ACKNOWLEDGMENTS

The authors gratefully acknowledge the patients whose clinical imaging data made this research possible, and whose experiences continue to inspire ongoing advances in neuro-oncologic imaging. We also thank the PET/MR technologists and clinical coordinators at both institutions for their dedication and expertise in supporting high-quality brain PET imaging. In particular, Dr. Ivanidze wishes to thank Nelson Duran, Bernard Ho, Douglas Calov, and Katie Jiang for their exceptional contributions to the WCM Brain PET program. Dr. Barajas thanks Bethany Barajas MSN for her helpful comments regarding this manuscript and dedicates this research to the memory of Rachel Dawn Gabani and Justin S Cetas, MD, PhD.

REFERENCES

1. Stupp R, Mason WP, van den Bent MJ, et al. Radiotherapy plus concomitant and adjuvant temozolomide for glioblastoma. *N Engl J Med*. Mar 10 2005;352(10):987-96. doi:10.1056/NEJMoa043330
2. Fu R, Szidonya L, Barajas RF, Jr., Ambady P, Varallyay C, Neuwelt EA. Diagnostic performance of DSC perfusion MRI to distinguish tumor progression and treatment-related changes: a systematic review and meta-analysis. *Neurooncol Adv*. Jan-Dec 2022;4(1):vdac027. doi:10.1093/noajnl/vdac027
3. Galldiks N, Lohmann P, Aboian M, et al. Update to the RANO working group and EANO recommendations for the clinical use of PET imaging in gliomas. *Lancet Oncol*. Aug 2025;26(8):e436-e447. doi:10.1016/S1470-2045(25)00193-7
4. Galldiks N, Lohmann P, Fink GR, Langen KJ. Amino Acid PET in Neurooncology. *J Nucl Med*. May 2023;64(5):693-700. doi:10.2967/jnumed.122.264859
5. Kondo A, Ishii H, Aoki S, et al. Phase IIa clinical study of [(18)F]fluciclovine: efficacy and safety of a new PET tracer for brain tumors. *Ann Nucl Med*. Nov 2016;30(9):608-618. doi:10.1007/s12149-016-1102-y
6. Wen PY, van den Bent M, Youssef G, et al. RANO 2.0: Update to the Response Assessment in Neuro-Oncology Criteria for High- and Low-Grade Gliomas in Adults. *J Clin Oncol*. Nov 20 2023;41(33):5187-5199. doi:10.1200/JCO.23.01059
7. Albert NL, Weller M, Suchorska B, et al. Response Assessment in Neuro-Oncology working group and European Association for Neuro-Oncology recommendations for the clinical use of PET imaging in gliomas. *Neuro Oncol*. Sep 2016;18(9):1199-208. doi:10.1093/neuonc/now058
8. Rosen J, Werner JM, Cecccon GS, et al. MRI and (18)F-FET PET for Multimodal Treatment Monitoring in Patients with Brain Metastases: A Cost-Effectiveness Analysis. *J Nucl Med*. Jun 3 2024;65(6):838-844. doi:10.2967/jnumed.123.266687
9. Rosen J, Werner JM, Cecccon GS, et al. Diagnosis of treatment-related changes in children and adolescents with brain and spinal tumors: a cost-effectiveness analysis using MRI and [18 F]FET PET. *Eur J Nucl Med Mol Imaging*. Jun 4 2025;doi:10.1007/s00259-025-07377-x
10. Mair MJ, Lohmann P, Galldiks N, et al. Availability and use of PET in patients with brain tumours - a European Organisation for Research and Treatment of Cancer - Brain Tumour Group (EORTC-BTG) survey. *Eur J Nucl Med Mol Imaging*. Jun 4 2025;doi:10.1007/s00259-025-07366-0
11. Bogsrud TV, Londalen A, Brandal P, et al. 18F-Fluciclovine PET/CT in Suspected Residual or Recurrent High-Grade Glioma. *Clin Nucl Med*. Aug 2019;44(8):605-611. doi:10.1097/RLU.0000000000002641
12. Nabavizadeh A, Bagley SJ, Doot RK, et al. Distinguishing Progression from Pseudoprogression in Glioblastoma Using (18)F-Fluciclovine PET. *J Nucl Med*. Jun 2023;64(6):852-858. doi:10.2967/jnumed.122.264812
13. Bossuyt PM, Reitsma JB, Bruns DE, et al. STARD 2015: an updated list of essential items for reporting diagnostic accuracy studies. *BMJ*. Oct 28 2015;351:h5527. doi:10.1136/bmj.h5527
14. Ellingson BM, Bendszus M, Boxerman J, et al. Consensus recommendations for a standardized Brain Tumor Imaging Protocol in clinical trials. *Neuro Oncol*. Sep 2015;17(9):1188-98. doi:10.1093/neuonc/nov095
15. Ellingson BM, Sanvito F, Cloughesy TF, et al. A Neuroradiologist's Guide to Operationalizing the Response Assessment in Neuro-Oncology (RANO) Criteria Version 2.0 for Gliomas in Adults. *AJNR Am J Neuroradiol*. Dec 9 2024;45(12):1846-1856. doi:10.3174/ajnr.A8396
16. Statistics Kingdom. (2017). Receiver Operating Characteristic Calculator. Accessed 8/20/25, 2025. https://www.statkingdom.com/410multi_linear_regression.html
17. Maurer GD, Brucker DP, Stoffels G, et al. (18)F-FET PET Imaging in Differentiating Glioma Progression from Treatment-Related Changes: A Single-Center Experience. *J Nucl Med*. Apr 2020;61(4):505-511. doi:10.2967/jnumed.119.234757
18. Cui M, Zorrilla-Veloz RI, Hu J, Guan B, Ma X. Diagnostic Accuracy of PET for Differentiating True Glioma Progression From Post Treatment-Related Changes: A Systematic Review and Meta-Analysis. *Front Neurol*. 2021;12:671867. doi:10.3389/fneur.2021.671867
19. Puranik AD, Dev ID, Rangarajan V, et al. FET PET to differentiate between post-treatment changes and recurrence in high-grade gliomas: a single center multidisciplinary clinic controlled study. *Neuroradiology*. Feb 2025;67(2):363-369. doi:10.1007/s00234-024-03495-9
20. Hope TEOB, N. A.; Raleigh, D.; Soloman, D.; Wilson, D., Dababo, N.; Barkovich, M.; Cade, D.; Mcconathy, J.; Johnson, D.; Langen, K.-J.;

- Villanueva-Meyer, J. Characterization of recurrent tumor and treatment related effect using 18F-Fluoroethytyrosine in gliomas: results from a prospective phase 2 trial (UC-GlioFET). *Journal of Nuclear Medicine*; 2025:
21. van Dijken BRJ, van Laar PJ, Holtman GA, van der Hoorn A. Diagnostic accuracy of magnetic resonance imaging techniques for treatment response evaluation in patients with high-grade glioma, a systematic review and meta-analysis. *Eur Radiol.* Oct 2017;27(10):4129-4144. doi:10.1007/s00330-017-4789-9
 22. Chen W. Clinical applications of PET in brain tumors. *J Nucl Med.* Sep 2007;48(9):1468-81. doi:10.2967/jnumed.106.037689
 23. Johnson JM, Chen MM, Rohren EM, et al. Delayed FDG PET Provides Superior Glioblastoma Conspicuity Compared to Conventional Image Timing. *Front Neurol.* 2021;12:740280. doi:10.3389/fneur.2021.740280
 24. de Zwart PL, van Dijken BRJ, Holtman GA, et al. Diagnostic Accuracy of PET Tracers for the Differentiation of Tumor Progression from Treatment-Related Changes in High-Grade Glioma: A Systematic Review and Metaanalysis. *J Nucl Med.* Apr 2020;61(4):498-504. doi:10.2967/jnumed.119.233809
 25. Brandes AA, Tosoni A, Spagnoli F, et al. Disease progression or pseudoprogression after concomitant radiochemotherapy treatment: pitfalls in neurooncology. *Neuro Oncol.* Jun 2008;10(3):361-7. doi:10.1215/15228517-2008-008
 26. Chao ST, Ahluwalia MS, Barnett GH, et al. Challenges with the diagnosis and treatment of cerebral radiation necrosis. *Int J Radiat Oncol Biol Phys.* Nov 1 2013;87(3):449-57. doi:10.1016/j.ijrobp.2013.05.015
 27. Galldiks N, Dunkl V, Stoffels G, et al. Diagnosis of pseudoprogression in patients with glioblastoma using O-(2-[18F]fluoroethyl)-L-tyrosine PET. *Eur J Nucl Med Mol Imaging.* Apr 2015;42(5):685-95. doi:10.1007/s00259-014-2959-4

SUPPLEMENTAL FILES

Supplementary Table S1: Standards for Reporting Diagnostic accuracy studies (STARD)-2015 checklist is provided to facilitate completeness and transparency of reporting in diagnostic accuracy studies.

Section & Topic	No	Item	Reported on page #
TITLE OR ABSTRACT			
	1	Identification as a study of diagnostic accuracy using at least one measure of accuracy (such as sensitivity, specificity, predictive values, or AUC)	Lines 1-41
ABSTRACT			
	2	Structured summary of study design, methods, results, and conclusions (for specific guidance, see STARD for Abstracts)	Lines 2-41
INTRODUCTION			
	3	Scientific and clinical background, including the intended use and clinical role of the index test	Lines 49-126
	4	Study objectives and hypotheses	Lines 126-136
METHODS			
<i>Study design</i>	5	Whether data collection was planned before the index test and reference standard were performed (prospective study) or after (retrospective study)	Line 141-157
<i>Participants</i>	6	Eligibility criteria	Lines 141-157
	7	On what basis potentially eligible participants were identified (such as symptoms, results from previous tests, inclusion in registry)	Lines 141-157
	8	Where and when potentially eligible participants were identified (setting, location and dates)	Line 141-157
	9	Whether participants formed a consecutive , random or convenience series	Line 145
<i>Test methods</i>	10a	Index test, in sufficient detail to allow replication	Lines 180-198
	10b	Reference standard, in sufficient detail to allow replication	Lines 188-198
	11	Rationale for choosing the reference standard (if alternatives exist)	Lines 188-198
	12a	Definition of and rationale for test positivity cut-offs or result categories of the index test, distinguishing pre-specified from exploratory	Lines 200-217
	12b	Definition of and rationale for test positivity cut-offs or result categories of the reference standard, distinguishing pre-specified from exploratory	Lines 200-217
	13a	Whether clinical information and reference standard results were available to the performers/readers of the index test	Line 186

<i>Analysis</i>	13b	Whether clinical information and index test results were available to the assessors of the reference standard	Line 186
	14	Methods for estimating or comparing measures of diagnostic accuracy	Line 200-217
	15	How indeterminate index test or reference standard results were handled	NA
	16	How missing data on the index test and reference standard were handled	NA
	17	Any analyses of variability in diagnostic accuracy, distinguishing pre-specified from exploratory	Line 200-217
RESULTS <i>Participants</i>	18	Intended sample size and how it was determined	NA
	19	Flow of participants, using a diagram	NA
	20	Baseline demographic and clinical characteristics of participants	Lines 200-236
	21a	Distribution of severity of disease in those with the target condition	Lines 200-236
	21b	Distribution of alternative diagnoses in those without the target condition	Lines 200-236
<i>Test results</i>	22	Time interval and any clinical interventions between index test and reference standard	Line 494
	23	Cross tabulation of the index test results (or their distribution)	Lines 238-260
	24	by the results of the reference standard Estimates of diagnostic accuracy and their precision (such as 95% confidence intervals)	Lines 246-26-
	25	Any adverse events from performing the index test or the reference standard	NA
DISCUSSION	26	Study limitations, including sources of potential bias, statistical uncertainty, and generalisability	Lines 383-394
	27	Implications for practice, including the intended use and clinical role of the index test	Lines 274-302
OTHER INFORMATION	28	Registration number and name of registry	NA
	29	Where the full study protocol can be accessed	NA
	30	Sources of funding and other support; role of funders	NA

Supplementary Table S2: MRI Parameters. TR= Repetition Time, TE= Echo Time, TI= Inversion Time, NEX= number of excitations or averages, FOV= Field of View, ms= milliseconds, IR-GRE inversion-recovery gradient-recalled echo, FSE= fast spin echo.

	Institution 1			Institution 2	
Sequence	3DT1 Post IR-GRE	3D T1 Post FSE	3D T2 FLAIR FSE	3D T1 Post FSE	3D T2 FLAIR FSE
Acquisition Plane	Axial	Axial	Sagittal	Sagittal	Sagittal
Mode	3D	3D	3D	3D	3D
TR [ms]	7.164	742	5000	700	7600
TE [ms]	2.868	12.29	105.7	19.0	386
TI [ms]	600	NA	1462	NA	2400
Flip Angle	9.0	90	90	>90	>90
NEX	1	1	1	1	1
FOV	256 mm	250 mm	250 mm	250 mm	250 mm
Slice Thickness	1 mm	.98 mm	.99 mm	1 mm	1.00 mm
Gap/Spacing	0	0	0	0	0

Supplementary Table S3: Diagnostic Performance of [F18]-Fluciclovine SUVmax for Differentiating Treatment Related Changes from Glioblastoma Progression. Reported as calculated value (95% confidence interval). AUC= Area Under the ROC Curve, LR+= Positive Likelihood Ratio, LR-= Negative Likelihood Ratio, PPV= Positive Predictive Value, NPV= Negative Predictive Value, NA= not applicable, please note positive likelihood ratio cannot be calculated when specificity = 1.

SUVmax Threshold	LR+	LR-	PPV	NPV
------------------	-----	-----	-----	-----

Combined	5.70	6.05 (2.38-2.05)	0.16 (0.01-0.36)	0.90 (0.76-0.99)	0.80 (0.57-0.99)
Nabavizade <i>et al</i> ⁸	4.66	3.18 (1.38-7.36)	0.13 (0.03-0.50)	0.83 (0.64-0.93)	0.83 (0.55-0.95)
Institution 1	8.64	NA	0.25 (0.12-0.74)	1.00 (0.66-1.00)	0.63 (0.31-0.86)
Institution 2	5.70	NA	0.20 (0.06-0.69)	1.00 (0.67-1.00)	0.82 (0.52-0.95)

Supplementary Table S4: [F18]-Fluciclovine SUVmax by Subgroup and Institution. Mean and standard deviation of SUVmax are provided along with p-values indicating statistical significance (Mann Whitney U test for group comparisons).

	Progression	Treatment-Related Changes	p-value
Combined	8.79 (3.72)	3.74 (2.07)	< .01
	N= 22	N= 14	
Institution 1	10.32 (4.07)	5.49 (1.84)	.02
	N= 12	N= 5	
Institution 2	6.97 (2.28)	2.77 (1.51)	< .01
	N= 10	N= 9	